Nonaqueous Synthesis of Mesostructured Aluminophosphate/Surfactant Composites: Synthesis, Characterization, and In-Situ SAXS Studies

M. Tiemann,[†] M. Fröba,*[,†] G. Rapp,[‡,§] and S. S. Funari[‡,||]

Institute of Inorganic and Applied Chemistry, University of Hamburg, Martin-Luther-King-Platz 6, D-20146 Hamburg, Germany, and European Molecular Biology Laboratory (EMBL), Outstation at Deutsches Elektronen-Synchrotron (DESY), Notkestrasse 85, D-22603 Hamburg, Germany

Received October 26, 1999. Revised Manuscript Received January 31, 2000

Mesostructured aluminophosphate/dodecyl phosphate composite materials were synthesized under aqueous and alcoholic conditions. The syntheses were monitored by temperature- and time-resolved in-situ small-angle X-ray scattering (SAXS). In the aqueous synthesis, a lamellar mesostructure is formed within the first few minutes of the reaction; this structure maintains a constant *d* spacing independent of the reaction time and temperature. The alcoholic synthesis at low temperature yields a mixture of a lamellar and a supposedly inverted hexagonal mesostructure. SAXS investigations show that these two phases evolve competitively. The lamellar structure is favored by higher temperatures and/or longer synthesis times; above ∼70 °C it is formed exclusively. Mixtures of both phases can be isolated as solid materials, but thermal analysis shows that the inverted hexagonal product transforms into the lamellar phase at ∼35−43 °C. The alcoholic synthesis is a highly cooperative reaction; the pure surfactant/alcohol systems are not lyotropic as long as the inorganic reactants are absent. In comparison, the surfactant/water system with the same surfactant concentrations as employed for the aqueous syntheses is lyotropic with a lamellar structure.

Introduction

The utilization of supramolecular assemblies of surfactant molecules as structure-directing templates has become a powerful and well-established method in the synthesis of ordered mesostructured materials. After its introduction in the synthesis of silica and aluminosilicate phases in 1992,[1] this approach has been extended to numerous other systems, like (transition) metal oxides[2−9] or chalcogenides.[10−14] In light of the significant role of zeolite analogous microporous aluminophosphates[15] ($AlPO_4$-*n*) and silicoaluminophosphates[16] (SAPO-*n*) in numerous catalytic applications,[17] it is obvious that there is also a high demand for similar materials with larger pores. Such mesoporous aluminophosphates have been reported recently.[18−22] Moreover, there have been several syntheses of mesostructured aluminophosphate/

* To whom correspondence should be addressed. Email: Froeba@xray.chemie.uni-hamburg.de.

[†] University of Hamburg.

[‡] European Molecular Biology Laboratory (EMBL).

[§] Current address: Max-Planck-Institute for Colloid and Interface Science, c/o Hamburger Synchrotronstrahlungslabor (HASYLAB) at Deutsches Elektronen-Synchrotron (DESY), Notkestrasse 85, D-22603 Hamburg, Germany.

[||] Current address: Department of Physics and Geosciences, University of Leipzig, c/o Hamburger Synchrotronstrahlungslabor (HASYLAB) at Deutsches Elektronen-Synchrotron (DESY), Notkestrasse 85, D-22603 Hamburg, Germany.

(1) (a) Kresge, C. T.; Leonowicz, M. E.; Roth, W. J.; Vartuli J. C.; Beck, J. S. *Nature* **1992**, *359*, 710−712. (b) Beck, J. S.; Vartuli, J. C.; Roth, W. J.; Leonowicz, M. E.; Kresge, C. T.; Schmitt, K. D.; Chu, C. T.-W.; Oloson, D. H.; Sheppard, E. W.; McCullen, S. B.; Higgins, J. B.; Schlenker, J. L. *J. Am. Chem. Soc.* **1992**, *114*, 10834−10843.

(2) Antonelli, D. M.; Ying, J. Y. *Angew. Chem., Int. Ed. Engl.* **1995**, *34*, 2014−2017.

(3) Ciesla, U.; Schacht, S.; Stucky, G. D.; Unger, K. K.; Schüth, F. *Angew. Chem., Int. Ed. Engl.* **1996**, *35*, 541−543.

(4) (a) Antonelli, D. M.; Ying, J. Y. *Angew. Chem., Int. Ed. Engl.* **1996**, *35*, 426−430. (b) Antonelli, D. M.; Nakahira, A.; Ying, J. Y. *Inorg. Chem.* **1996**, *35*, 3126−3136.

(5) Fröba, M.; Muth, O.; Reller, A. *Solid State Ionics* **1997**, *101−103*, 249−253.

(6) Tian, Z.-R.; Tong, W.; Wang, J.-Y.; Duan, N.-G.; Krishnan, V. V.; Suib, S. L. *Science* **1997**, *276*, 926−930.

(7) Wong, M. S.; Ying, J. Y. *Chem. Mater.* **1998**, *10*, 2067−2077.

(8) Fröba, M.; Muth, O. *Adv. Mater.* **1999**, *11*, 564−567.

(9) Ciesla, U.; Fröba, M.; Stucky, G. D.; Schüth, F. *Chem. Mater.* **1999**, *11*, 227−234.

(10) Fröba, M.; Oberender, N. *Chem. Commun.* **1997**, 1729−1730.

(11) Bonhomme, F.; Kanatzidis, M. G. *Chem. Mater.* **1998**, *10*, 1153−1159.

(12) Neeraj; Rao, C. N. R. *J. Mater. Chem.* **1998**, *8*, 279−280.

(13) MacLachlan, M. J.; Coombs, N.; Ozin, G. A. *Nature* **1999**, *397*, 681−684.

(14) (a) Braun, P. V.; Osenar, P.; Stupp, S. I. *Nature* **1996**, *380*, 325−328. (b) Tohver, V.; Braun, P. V.; Pralle, M. U.; Stupp, S. I. *Chem. Mater.* **1997**, *9*, 1495−1498. (c) Braun, P. V.; Osenar, P.; Tohver, V.; Kennedy, S. B.; Stupp, S. I. *J. Am. Chem. Soc.* **1999**, *121*, 7302−7309.

(15) Wilson, S. T.; Lok, B. 1 M.; Messina, C. A.; Cannan, T. R.; Flanigen, E. M. *J. Am. Chem. Soc.* **1982**, *104*, 1146−1147.

(16) Lok, B. M.; Messina, C. A.; Patton, R. L.; Gajek, R. T.; Cannan, T. R.; Flanigen, E. M. *Am. Chem. Soc.* **1984**, *106*, 6092−6093.

(17) Hartmann, M.; Kevan, L. *Chem. Rev.* **1999**, *99*, 635−663.

(18) (a) Zhao, D.; Luan, Z.; Kevan, L. *Chem. Commun.* **1997**, 1009−1010. (b) Luan, Z.; Zhao, D.; He, H.; Klinowski; J.; Kevan, L. *J. Phys. Chem. B* **1998**, *102*, 1250−1259.

(19) Holland, B. T.; Isbester, P. K.; Blanford, C. F.; Munson E. J.; Stein, A. *J. Am. Chem. Soc.* **1997**, *119*, 6796−6803.

(20) (a) Kimura, T.; Sugahara, Y.; Kuroda, K. *Chem. Commun.* **1998**, 559−560. (b) *Microporous Mesoporous Mater.* **1998**, *22*, 115−126. (c) *Chem. Mater.* **1999**, *11*, 508−518.

(21) Cabrera, S.; Haskouri, J. E.; Guillem, C.; Beltrán-Porter, A.; Beltrán-Porter, D.; Mendioroz, S.; Marcos, M. D.; Amorós, P. *Chem. Commun.* **1999**, 333−334.

10.1021/cm991165d CCC: $19.00
Published on Web 04/26/2000

surfactant composites,[23−28] which did not lead to porous materials, since the surfactant could not be removed without collapse of the structure; nevertheless, these products are still of interest for structural investigations and mechanistic studies. In most cases the preparations of the above-mentioned materials were carried out in aqueous systems under hydrothermal conditions; some also employed tetraethylene glycol and/or unbranched primary alcohols instead of water.[23,25]

There have been several discussions on the reaction mechanisms that are involved in the template-directed synthesis of mesostructured materials;[1,29−32] however, in-situ investigations on these reactions have so far been restricted to silica phases prepared in aqueous media. Extensive investigations in this field were performed by Firouzi et al.,[33] who employed a variety of characterization methods, such as small-angle X-ray (SAXS) and neutron (SANS) scattering, polarized light optical microscopy (POM), and NMR spectroscopy (^{2}H, ^{13}C, ^{29}Si, ^{81}Br). Apart from investigating the cooperative organization of silicate anions and/or oligomers with cetyltrimethylammonium bromide surfactant into nanostructured assemblies, they also studied the phase behavior of a "passive" liquid-crystalline model system containing both the surfactant and the silicate species, in which the polymerization of the silicate is suppressed by highly alkaline conditions. In comparison, Rathouský et al.[34] have recently investigated the formation of mesostructured silica from a similar synthesis mixture using X-ray diffraction; their system is not lyotropic in the passive state (at high pH) and the mesostructure evolves only after acidification, i.e., after the start of the silicate polymerization. O'Brien et al.[35] have studied the synthesis of silica mesostructures by time-resolved synchrotron X-ray diffraction, focusing particularly on the effect of using different silica sources. High time−resolution kinetic investigations were carried out by Lindén and Ågren et al.,[36] who used in-situ synchrotron X-ray diffraction in a specific tubular reactor and observed the structure formation of MCM-41 type silica phases as early as 3 min after the start of the reaction; they also studied the influence of cosurfactants. Calabro et al.[37] have employed ATR/FTIR spectroscopy to simultaneously study the changes and synergies in both the lyotropic phase in the synthesis mixture and the solid product.

Experimental Section

Aluminophosphate/surfactant composite materials were prepared from aluminum triisopropoxide (Al[O^{i}Pr]$_3$, Merck), phosphoric acid (H_3PO_4, 85%, Fluka), and monododecyl phosphate ($C_{12}H_{25}OPO(OH)_2$; in the following: C_{12}−PO_4, Lancaster). A mixture of the surfactant and the respective solvent was homogenized by stirring at room temperature (ethanol, methanol) or 50 °C (water), respectively. Equal amounts of Al[O^{i}Pr]$_3$ and H_3PO_4 were then added at room temperature followed by 10 min stirring. (Alcoholic solutions contained ∼5% water.) In a typical synthesis, the molar composition of the reaction mixture was $C_{12}PO_4$/Al(O^{i}Pr)$_3$/H_3PO_4/solvent = 1/1/1/50. The mixture was kept for 12−24 h at the desired reaction temperature in closed glass tubes or Teflon-lined autoclaves, respectively. The solid products were filtered off, washed with ethanol, and dried under vacuum.

Temperature- and time-resolved small-angle X-ray scattering (SAXS) investigations were carried out at the European Molecular Biology Laboratory (EMBL), Outstation at Deutsches Elektronen-Synchrotron (DESY), Hamburg, Germany, beamline X 13. The samples were placed in the X-ray beam in flame-sealed glass capillaries of 1 mm diameter. Investigations on samples containing the inorganic species were carried out within 5−10 min after the addition of Al[O^{i}Pr]$_3$ and H_3PO_4 to the surfactant/solvent mixture. For temperature-resolved measurements the following procedure was used: 4 min heating (by 20 °C at 5 °C/min), 3 min temperature equilibration, 4 min data collection. Diffraction patterns were recorded with a 1024 channel linear detector.[38] Data processing was carried out with OTOKO software;[39] diffraction peak positions were calibrated against silver behenate (d_{001} = 5.8380(3) nm)[40] and transformed for clarity into a 2θ scaling based on the wavelength of Cu Kα radiation (0.15405 nm).

Powder X-ray diffraction (PXRD) patterns were recorded on a Philips PW 1050/25 diffractometer using filtered Cu Kα radiation. Simultaneous thermogravimetry, differential thermal analysis, and mass spectrometry (TG/DTA/MS) was performed on a Netzsch STA 409 thermobalance coupled with a Baltzer QMG 421 quadrupole mass spectrometer (multiple ion detection method). Differential scanning calorimetry (DSC) was carried out with a Mettler DSC 27 HP calorimeter. For all thermal analyses, the samples were heated at 5 K/min in open crucibles under air atmosphere (controlled air flow for TG/DTA/MS). Polarized light optical microscopy (POM) was carried out with an Olympus BX50 microscope and a Mettler Toledo FP82HT heating stage.

Results and Discussion

Aqueous Synthesis. The aqueous synthesis of nanostructured aluminophosphate/dodecyl phosphate com-

(22) Eswaramoorthy, M.; Neeraj, S.; Rao, C. N. R. *Microporous Mesoporous Mater.* **1999**, *28*, 205−210.
(23) (a) Oliver, S.; Coombs, N.; Ozin, G. A. *Adv. Mater.* **1995**, *7*, 931−935. (b) Oliver, S.; Kuperman, A.; Coombs, N.; Lough A.; Ozin, G. A. *Nature* **1995**, *378*, 47−50.
(24) (a) Sayari, A.; Karra, V. R.; Reddy, J. S.; Moudrakovski, I. L. *Chem. Commun.* **1996**, 411−412. (b) Chenite, A.; Le Page Y.; Karra, V. R.; Sayari, A. *Chem. Commun.* **1996**, 413−414. (c) Sayari, A.; Moudrakovski, I.; Reddy, J. S. *Chem. Mater.* **1996**, *8*, 2080−2088.
(25) (a) Gao, Q.; Xu, R.; Chen, J.; Li, R.; Li, S.; Qui, S.; Yue, Y. *J. Chem. Soc., Dalton Trans.* **1996**, 3303−3307. (b) Gao, Q.; Chen, J.; Xu, R.; Yue, Y. *Chem. Mater.* **1997**, *9*, 457−462.
(26) Feng, P.; Xia, Y.; Feng, J.; Bu, X.; Stucky, G. D. *Chem. Commun.* **1997**, 949−950.
(27) Fröba, M.; Tiemann, M. *Chem. Mater.* **1998**, *10*, 3475−3483.
(28) (a) Khimyak, Y. Z.; Klinowski, J. *Chem. Mater.* **1998**, *19*, 2258−2265. (b) Khimyak, Y. Z.; Klinowski, J. *J. Chem. Soc., Faraday Trans.* **1998**, *94*, 2241−2247.
(29) Beck, J. S.; Vartuli, J. C.; Kennedy, G. J.; Kresge, C. T.; Roth, W. J.; Schramm, S. E. *Chem. Mater.* **1994**, *6*, 1816−1821.
(30) (a) Huo, G.; Margolese, D. I.; Ciesla, U.; Feng, P.; Gier, T. E.; Sieger, P.; Leon, R.; Petroff, P. M.; Schüth, F.; Stucky, G. D. *Nature* **1994**, *368*, 317−321. (b) Huo, Q.; Margolese, D. I.; Ciesla, U.; Demuth, D. G.; Feng, P.; Gier, T. E.; Sieger, P.; Firouzi, A.; Chmelka, B. F.; Schüth, F.; Stucky, G. D.; *Chem. Mater.* **1994**, *6*, 1176−1191.
(31) Tanev, P. T.; Pinnavaia, T. J. *Chem. Mater.* **1996**, *8*, 2068−2079.
(32) Behrens, P. *Angew. Chem., Int. Ed. Engl.* **1996**, *35*, 515−518.
(33) (a) Firouzi, A.; Kumar, D.; Bull, L. M.; Besier, T.; Sieger, P.; Huo, Q.; Walker, S. A.; Zasadzinski, J. A.; Glinka, C.; Nicol, J.; Margolese, D.; Stucky, G. D.; Chmelka, B. F. *Science* **1995**, *267*, 1138−1143. (b) Firouzi, A.; Atef, F.; Oertli, A. G.; Stucky, G. D.; Chmelka, B. F. *J. Am. Chem. Soc.* **1997**, *119*, 3596−3610.
(34) Rathouský, J.; Schulz-Ekloff, G.; Had, J.; Zukal, A. *Phys. Chem. Chem. Phys* **1999**, *1*, 3053−3057.
(35) (a) O'Brien, S.; Francis, R. J.; Price, S. J.; O'Hare, D.; Clark, S. M.; Okazaki, N.; Kuroda, K. *J. Chem. Soc., Chem. Commun.* **1995**, 2423−2424. (b) O'Brien, S.; Francis, R. J.; Fogg, A.; O'Hare, D.; Okazaki, N.; Kuroda, K. *Chem. Mater.* **1999**, *11*, 1822−1832.
(36) (a) Lindén, M.; Schunk, S. A.; Schüth, F. *Angew. Chem., Int. Ed. Engl.* **1998**, *37*, 821−823. (b) Ågren, P.; Lindén, M.; Rosenholm, J. B.; Schwarzenbacher, R.; Kriechbaum, M.; Amenitsch, H.; Laggner, P.; Blanchard, J.; Schüth, F. *J. Phys. Chem. B* **1999**, *103*, 5943−5948.
(37) Calabro, D. C.; Valyocsik, E. W.; Ryan, F. X. *Microporous Mater.* **1996**, *7*, 243−259.
(38) Gabriel, A. *Rev. Sci. Instrum.* **1977**, *48*, 1303−1305.
(39) Boulin, C.; Kempf, R.; Koch, M. H. J.; McLaughlin, S. M. *Nucl. Instr. Methods Phys. Res. A* **1986**, *249*, 399−407.
(40) Huang, H.; Toraya, H.; Blanton, T. N.; Wu, Y. *J. Appl. Crystallogr.* **1993**, *26*, 180−184.

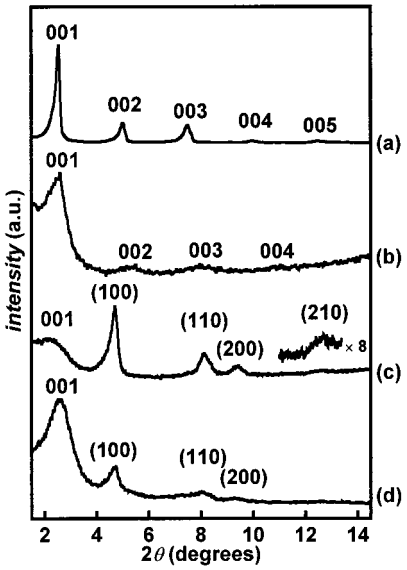

Figure 1. Powder X-ray diffraction diagrams of mesostructured aluminophosphate/dodecyl phosphate composite materials prepared under various conditions: (a) water, 120 °C; (b) ethanol, 90 °C; (c) ethanol, 10 °C; and (d) methanol, 25 °C. Lamellar phases and hexagonal phases (in parentheses) are indexed.

posite materials yields lamellar phases with d_{001} values between 3.5 and 3.7 nm. Raising the synthesis temperature within the region 20−120 °C and/or expanding the duration of the reaction within the range 12−72 h leads to a better quality of the powder X-ray diffraction (PXRD) patterns, i.e., an increase of the degree of order in the products. However, the interlamellar distances of the products are not affected by these synthesis parameters. The PXRD diagram of a sample product synthesized in water at 120 °C (30% w/w surfactant) is shown in Figure 1a (d_{001} = 3.47 nm). (A detailed characterization of lamellar aluminophosphates synthesized under aqueous conditions comprising thermal analysis and X-ray absorption spectroscopy[27] as well as solid-state NMR spectroscopy[41] is reported elsewhere.)

The effect of the reaction temperature is evident from in-situ small-angle X-ray scattering (SAXS) studies; Figure 2 shows the thermal evolution of a synthesis mixture containing equal amounts of C_{12}−PO_4, Al[O^{i}Pr]$_3$, and H_3PO_4 in water with a surfactant concentration of 30% w/w. The intensities of the 00*l* peaks grow with increasing temperature without any notable peak narrowing (the full widths at half-maximum remain basically constant), which suggests that a more condensed structure develops as the reaction temperature is raised. However, the peak positions (d_{001} = 3.61 nm) remain constant. In comparison, a sample which is kept constantly at 20 °C over the same time period as for the temperature-dependent measurements (∼45 min) exhibits no such change in the peak intensities. Hence, it may be concluded that an increase of temperature leads to a more complete reaction extend and, thus, to a higher density in the structure, but does not affect the interlamellar distances; this is consistent with the above-mentioned effect of the synthesis temperature on the final solid products as evidenced by PXRD.

(41) Schulz, M.; Tiemann, M.; Fröba, M.; Jäger, C. *J. Phys. Chem. B*, submitted for publication.

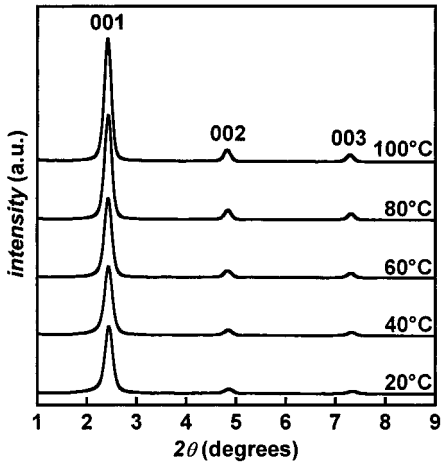

Figure 2. Thermal evolution of the SAXS diagrams of the aqueous synthesis mixture: C_{12}−PO_4/water (30/70 w/w), Al[O^{i}Pr]$_3$, H_3PO_4. (Equimolar amounts of C_{12}−PO_4, Al[O^{i}Pr]$_3$, and H_3PO_4.) The lamellar mesophase is indexed; d_{001} = 3.61 nm.

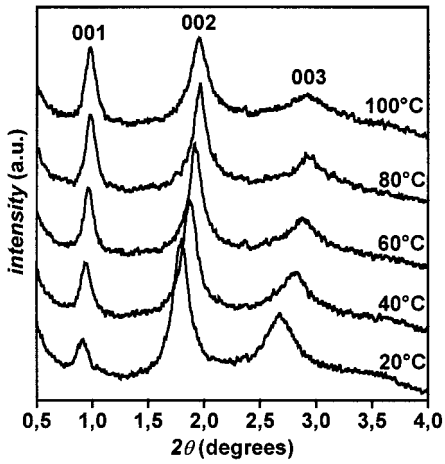

Figure 3. Thermal evolution of the SAXS diagrams of the system C_{12}−PO_4/water (30/70 w/w). The lamellar lyotropic phase is indexed; d_{001} = 9.83 nm (20 °C).

In comparison, temperature-resolved SAXS patterns of the pure C_{12}−PO_4/water system without the inorganic species (with the same surfactant concentration of 30% w/w) are shown in Figure 3. The system is lyotropic with a lamellar structure over the entire temperature region from 20 to 100 °C. This is also confirmed by polarized light optical microscopy (POM); Figure 4 shows a picture taken at 30 °C, in which the cross-shaped texture typical of lamellar liquid-crystalline phases is visible. In the pure surfactant/water system the interlamellar distance is considerably larger than in the system containing the inorganic reactants, which is explained by the presence of high amounts of water between the adjacent surfactant bilayers in a 30% (w/w) sample. The d_{001} value is 9.83 nm at 20 °C and reduces to 9.02 nm at 100 °C; this is caused by a shrinkage of the surfactant bilayers due to stronger Brownian lateral oscillation of the hydrophobic surfactant chains. The reflections are much broader and weaker than in the case of the mesostructure containing the inorganic species, which is explained by fluctuations of the interlayer distance, which, in turn, is less well-defined.[42]

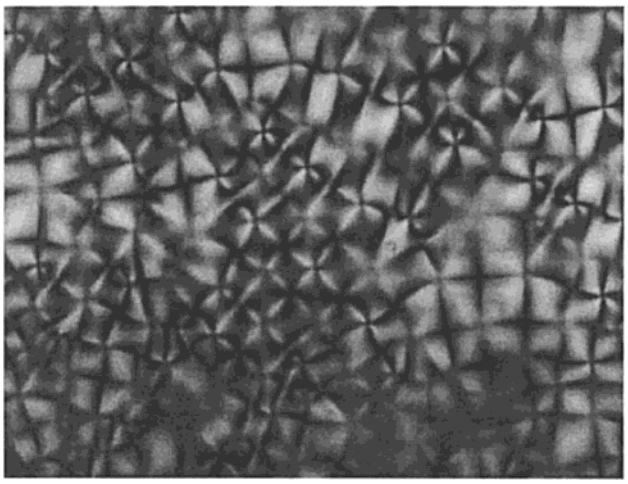

Figure 4. Polarized optical micrograph (POM) of the system $C_{12}-PO_4$/water (30/70 w/w) at 30 °C. The cross-shaped texture is typical of a lamellar lyotropic phase.

It must be pointed out that the SAXS data of the synthesis mixture (see Figure 2) were collected immediately after the addition of the inorganic reactants ($Al[O^iPr]_3$ and H_3PO_4) to the surfactant/water system (5−10 min, see Experimental Section). Therefore, two significant features must be stressed in terms of the time scale of these investigations: (i) Once the inorganic reactants are added, the lamellar structure with the small interlamellar distance ($d_{100} = 3.61$ nm), which is comparable to that of the final solid products obtained from the synthesis ($d_{100} = 3.47$ nm), forms within these first few minutes of the reaction without any further changes, apart from the quality of order. The d_{001} value is drastically diminished, which means that most of the water is immediately removed from the regions between the surfactant bilayers. (ii) The interlamellar distance is virtually independent of the temperature. Thus, it may be concluded that from the beginning on, the inorganic building units are already interconnected with each other to some degree; otherwise a swelling of the lamellae at higher temperatures would be expected, caused by an increased thermal movement of the individual (noninterconnected) inorganic units. Any temperature-induced swelling is only to be expected in the inorganic part rather than in the organic, i.e., hydrophobic part. Also, a swelling between one organic layer and the adjacent inorganic layer (at the organic/inorganic boundary) can only be expected as long as the inorganic units are not yet interconnected with each other. In this context it should also be mentioned that the interaction between the inorganic layer and the surfactant headgroups is of a covalent nature.[41] Such a temperature-dependent shift in the SAXS reflections is observed in the nonaqueous syntheses as will be discussed below.

On the other hand, it is important to note that at this early stage of the reaction no structured solid material can be isolated from the synthesis mixture yet; the complete condensation of the reactants, i.e., the formation of a fully developed solid network, requires several hours, depending on the temperature. Accordingly, the mutual interactions between the inorganic building units, the surfactant headgroups, and the remaining water molecules are strong enough to provide a certain rigidity in the mesostructure, but the formation of the final aluminophosphate layers with exclusively covalent Al−O−P bonds has by far not been completed yet.

Nonaqueous Synthesis. Similar lamellar mesostructures are obtained when the synthesis is carried out in ethanol or methanol, respectively, at temperatures of ∼70−90 °C (solvothermal conditions, i.e., at temperatures near or above the boiling point of the respective solvent). However, these products are considerably less well-defined than those from the aqueous syntheses; the PXRD pattern of a product prepared in ethanol at 90 °C ($d_{001} = 3.50$ nm) is shown in Figure 1b. The pure surfactant/alcohol solutions are optically isotropic, i.e., nonbirefringent under polarized light, and do not show any SAXS reflections over the entire temperature range (20−90 °C) and concentration region (5−50% w/w) studied, which means that the organization into a mesostructure occurs only after the addition of $Al[O^iPr]_3$ and H_3PO_4. This is an example of a highly cooperative synthesis of mesostructured materials. Both the relatively poor order of the products and the lack of any mesoscopic structure in the absence of the inorganic components are consistent with the fact that the alcohols have a considerably lower polarity than water (i.e., lower dielectric constants; at 25 °C, $\epsilon_{water} = 78$, $\epsilon_{methanol} = 33$, $\epsilon_{ethanol} = 24$); thus, the self-aggregation of the surfactant molecules into micelles is relatively disfavored in these alcohols compared to water.

Different products are obtained when the alcoholic synthesis is carried out at low temperatures (10−70 °C); the PXRD diagrams of two examples prepared in ethanol at 10 °C and methanol at 25 °C (both 20% w/w surfactant) are shown in Figure 1, parts c and d, respectively. In both cases the reflections are attributable to two distinct nanostructured phases, one of which has a clearly hexagonal structure with a remarkably low d_{100} value of 1.88 nm (corresponding to a lattice parameter of $a = 2 \cdot d_{100}/\sqrt{3} = 2.17$ nm), which will be discussed in detail below. The structure of the other phase cannot be identified from these diffraction patterns, but SAXS investigations (see below) suggest a lamellar phase. (Given the fact that the second- and third-order reflections of the lamellar product synthesized from the same system at a higher temperature are relatively weak (see Figure 2b), it is likely that this phase has the same lamellar structure with higher order reflections too weak to be detected.) The two mesophases evolve competitively; their relative amounts are systematically dependent on both the synthesis temperature and the reaction time. The lamellar phase is relatively favored at higher temperatures (and is exclusively formed above ∼70 °C, as shown above). This is seen in Figure 5 for products prepared in ethanol (20% w/w surfactant) at various temperatures (syntheses duration 12 h); these samples (A−D) will be further characterized below. A similar evolution is found for products synthesized at a constant temperature but with variable duration of the reaction; the reflection of the lamellar phase becomes more dominant while those of the hexagonal phase become weaker when the reaction is allowed to take place over a longer time period.

(42) Detailed SAXS investigations on the dodecyl phosphate/water system are to be published.

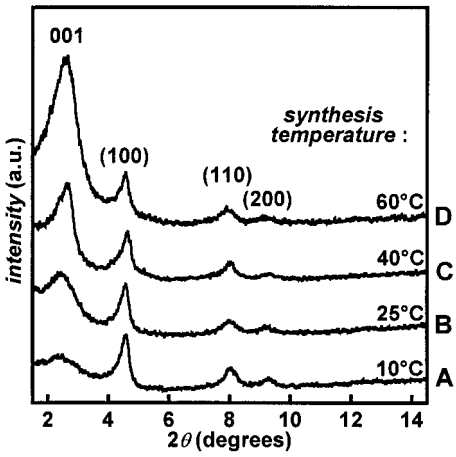

Figure 5. Powder X-ray diffraction diagrams of mesostructured aluminophosphate/dodecyl phosphate composite materials prepared in ethanol at various temperatures. The lamellar phase and the hexagonal phase (in parentheses) are indexed.

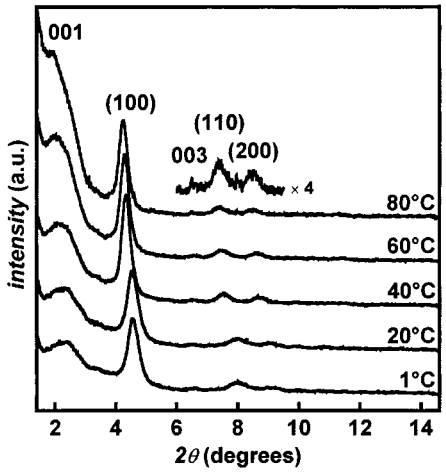

Figure 6. Thermal evolution of the SAXS diagrams of the alcoholic synthesis mixture: $C_{12}-PO_4$/ethanol (20/80 w/w), $Al[O^iPr]_3$, H_3PO_4. (Equimolar amounts of $C_{12}-PO_4$, $Al[O^iPr]_3$, and H_3PO_4.) The lamellar phase and the hexagonal phase (in parentheses) are indexed.

The influence of both the temperature and the reaction time on the relative amounts of the two phases is also evident from in-situ SAXS studies. Figure 6 displays the SAXS patterns of a synthesis mixture in ethanol (20% w/w surfactant) at variable temperatures; upon heating the 001 reflection of the lamellar phase grows in intensity relative to those of the hexagonal phase. (Note that in these diffraction patterns the 003 reflection of the lamellar phase is visible, whereas the 002 reflection overlaps with the 100 reflection of the hexagonal phase.) In this series a thermally induced shift of all reflections is observed. The *d* values of both the lamellar and the hexagonal phases slightly increase upon raising the temperature, which may be explained by an increased thermal oscillation of the inorganic building units that are at this point not yet interconnected with each other to a significant degree. This was not observed for the respective aqueous system (see Figure 2). The degree of condensation of the inorganic reactants into a rigid solid network at this early stage of the reaction is obviously much lower in alcohols than in water, which is to be expected in the light of a much slower hydrolysis of $Al[O^iPr]_3$.

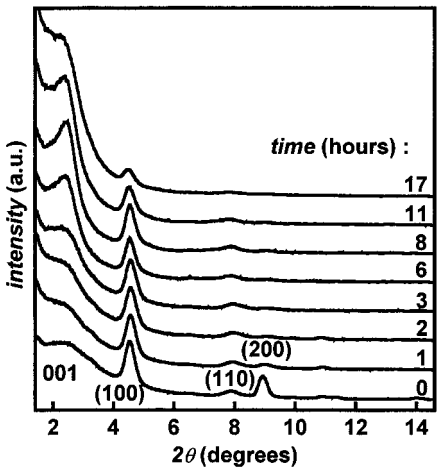

Figure 7. Temporal evolution of the SAXS diagrams of the alcoholic synthesis mixture: $C_{12}-PO_4$/ethanol (20/80 w/w), $Al[O^iPr]_3$, H_3PO_4. (Equimolar amounts of $C_{12}-PO_4$, $Al[O^iPr]_3$, and H_3PO_4.) The lamellar phase and the hexagonal phase (in parentheses) are indexed.

The temporal evolution of the SAXS patterns of a synthesis mixture with the same composition (20% w/w surfactant) at constantly 25 °C is shown in Figure 7; the lamellar phase becomes more and more dominant in the course of time. This progressive formation of the lamellar structure takes place on approximately the same time scale as the condensation of the inorganic reactants into a solid network. As a possible explanation of this correlation it may be assumed that the hexagonal arrangement is progressively disfavored with an increasing degree of condensation of the reactants; the successive formation of larger inorganic fragments in the course of the reaction may lead to a preferred mesostructured arrangement without curvature.

Characterization of the Hexagonal Mesostructure. The investigation of the hexagonal phase obtained from the nonaqueous low-temperature synthesis reveals some significant properties that are not typical of the usual hexagonal inorganic mesostructures prepared by this kind of synthesis. In the latter, the surfactant molecules are arranged in rodlike assemblies with the polar headgroups facing outward; the inorganic solid is structured around these micelles, forming a three-dimensional network (Figure 8a). (The term "three-dimensional" must be used with care; a hexagonal liquid crystal has a two-dimensional structure, as no crystallographic information is obtained regarding the direction along the surfactant rods. However, a solid-state mesostructured network with this symmetry is here referred to as three-dimensional in the sense that the building units are interconnected with each other in all three directions. With the same reasoning a lamellar solid mesostructure may be denoted as two-dimensional, although its crystallographic symmetry is one-dimensional.) In mesostructured inorganic/surfactant composite materials with this kind of hexagonal structure the d_{100} values are usually found to be in the region between 3 and 4 nm (for C_{12}-surfactants).[9,43−45] Contrary to that, the hexagonal structure in the system studied

(43) (a) Yada, M.; Machida, M.; Kijima, T. *Chem. Commun.* **1996**, 769−770. (b) Yada, M.; Takenaka, H.; Machida, M.; Kijima, T. *J. Chem. Soc., Dalton Trans.* **1998**, 1547−1550.

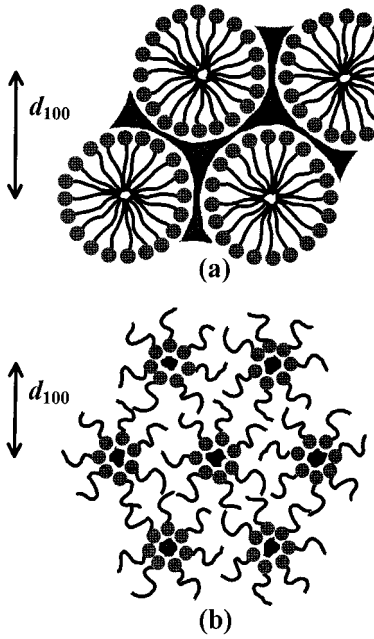

Figure 8. Schematic representation of two different hexagonal mesostructured inorganic/surfactant composites (cross section through the *hk* plane): (a) the normal structure with a fully connected inorganic network (drawn as dark area); and (b) inverted surfactant assemblies with single inorganic domains (dark areas) in the centers. In the latter case the diameters of the assemblies (and thus the d_{100} value) are smaller, since each hydrophobic surfactant chain is allowed more space for its distribution leading to a smaller radial extension; also, some degree of interpenetration of the chains from adjacent surfactant assemblies is possible.

here has a d_{100} value which is surprisingly low (1.88 nm), even if the possibility is taken into account that the phosphate headgroups from the surfactant may be considered as being part of the inorganic matrix, which might slightly diminish the d_{100} value as was shown by Fröba and Tiemann.[27] Therefore, a different hexagonal surfactant arrangement is suggested here as an alternative structure model, in which the surfactant molecules are assembled in an inverted arrangement, i.e., the polar headgroups are located inside of the rods and the hydrophobic chains are turned outward (Figure 8b). In this case the inorganic part is encapsulated in the centers of these assemblies forming individual domains that are not interconnected with each other and extend in one direction only.

Such an inverted hexagonal structure is very rarely observed in pure binary single-chain surfactant/solvent systems. Because of the geometry of these surfactant molecules (one thin hydrophobic chain and a spacious headgroup) and because of repulsion forces between the surfactant headgroups the inverted curvature is usually avoided; micelles, lamellae or structures with noninverted curvatures are favored. (However, if two or three hydrophobic chains are attached to each headgroup, as in biologically relevant phospholipids, inverted hexagonal phases are observed quite frequently.) In the system studied here, the emergence of the inverted structure may be explained by the presence of the inorganic reactants ($Al[O^iPr]_3$ and H_3PO_4). Owing to the interactions of the surfactant headgroups with the polar inorganic units the headgroup repulsion is reduced, which enables the inverted curvature. A similar effect, i.e., the formation of an inverted phase due to interactions of polar additives with the headgroups, was also observed by Funari[46] in the ternary system phospholipid/alkyl-polyoxyethylene/water. It should again be stressed that in the system $C_{12}-PO_4$/alcohol no lyotropic behavior is observed in the absence of the inorganic components.

This inverted structure provides a plausible explanation to the remarkably small d_{100} value, which can be accounted for by the fact that in such a structure there is more space available to each individual hydrophobic surfactant chain than in the noninverted structure, leading to a reduced radial extension (see Figure 8). Also, the micelles may be interpenetrating each other. It must be mentioned, however, that even in noninverted micelles, the arrangement of the hydrophobic chains is not necessarily rigidly linear, i.e., in an all-trans configuration, as may be implied by the schematic representation in Figure 8a. The diameter of noninverted rodlike micelles is already smaller than double the length of the linear (all-trans) surfactant molecule. Bearing in mind, however, that all previously reported (noninverted) hexagonal mesostructured inorganic/surfactant composite materials (with C_{12}-surfactants) had much larger d_{100} values than the structure studied here, the low value of the latter may be considered as a strong indication for the inverted structure.

Attempts to remove the surfactant without collapse of the structure (e.g., by solvent extraction) to obtain a porous aluminophosphate have failed. The structure is thermally extremely unstable; at temperatures above ~35 °C the solid products will irreversibly transform into single lamellar phases as is found by PXRD (not shown). This phase transformation will be discussed below. The poor thermal stability fits in with the inverted structure model, as it is consistent with an inorganic network that does not extend in all directions.

The solid mesostructured samples A−D (see Figure 5) consisting of the two phases were investigated by thermal analysis. Figure 9 shows the thermogravimetry/differential thermal analysis/mass spectrometry (TG/DTA/MS) diagram of sample A as an example. The endothermic decomposition of the surfactant occurs in one relatively sharp step at ~230−280 °C; H_2O^+, CO_2^+, and several organic mass fragments are detected ($C_2H_3^+$ and $C_4H_9^+$ shown exemplarily). The decomposition of the surfactant within such a narrow temperature interval indicates that the phosphate headgroups are not incorporated in the aluminophosphate matrix.[27] Prior to that (~50−120 °C) the removal of water is observed (5% endothermic mass loss). Below 50 °C, an endothermic peak is found in the DTA which is not accompanied by any mass loss; this corresponds to the phase transition of the inverted hexagonal into the lamellar phase. The TG/DTA/MS diagrams of the other three samples (B−D) are very similar. The relative mass loss caused by the decomposition of the surfactant varies systemati-

(44) (a) Antonelli, D. M.; Nakahira, A.; Ying, J. Y. *Inorg. Chem.* **1996**, *35*, 3126−3136. (b) Wong, M. S.; Ying, J. Y. *Chem. Mater.* **1998**, *10*, 2067−2077.

(45) Stone, V. F., Jr.; Davis, R. J. *Chem. Mater.* **1998**, *10*, 1468−1474.

(46) Funari, S. S. *Eur. Biophys. J.* **1998**, *27*, 590−594.

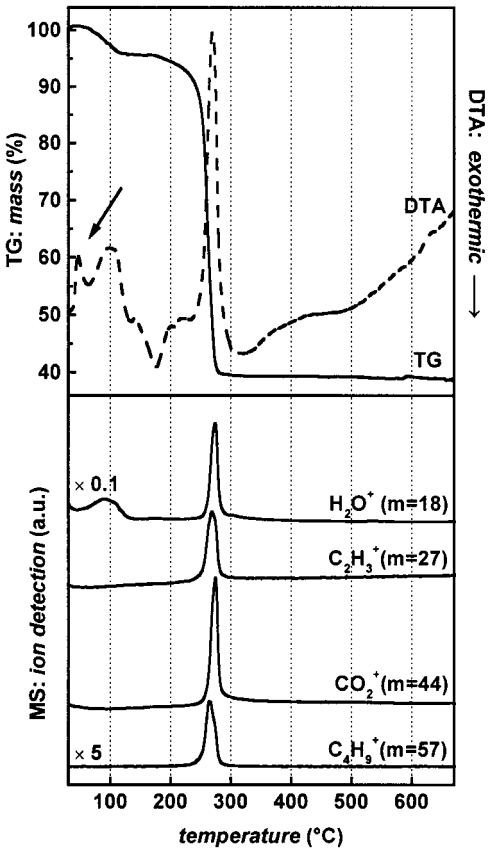

Figure 9. Thermal analysis (TG/DTA/MS) diagram of a mesostructured aluminophosphate/dodecyl phosphate composite prepared in ethanol at 10 °C (sample A, see Figure 5). The arrow indicates the phase transition of the hexagonal phase to the lamellar phase.

Table 1. Thermogravimetric Data of the Surfactant Decomposition and Calorimetric Data of the Phase Transition (Hexagonal-Lamellar) in the Samples A−D (See Figure 5)

		phase transition: calorimetric data		
sample	mass loss[a] (%)	θ_{onset} (°C)	θ_{offset} (°C)	enthalpy[b] (J/g)
A	58.1	35.8	42.6	58.0
B	50.4	35.2	40.9	37.4
C	47.8	35.5	40.4	24.0
D	44.2	34.8	39.6	11.3

[a] During surfactant decomposition. [b] Peak integration.

cally with the relative amount of the hexagonal phase in the respective sample: The higher the relative intensities of the PXRD reflections from the hexagonal phase are (A > B > C > D, see Figure 5), the greater is the mass loss detected by TG. This is shown in Table 1; the mass losses are calculated relative to the masses of the samples at 150 °C, i.e., after the initial removal of water. This correlation indicates that the amount of surfactant relative to the amount of inorganic material is larger for the inverted hexagonal than for the lamellar phase.

The phase transition from inverted hexagonal to lamellar, as detected by DTA, was also monitored quantitatively by differential scanning calorimetry (DSC). As expected, the enthalpy of this transition with respect

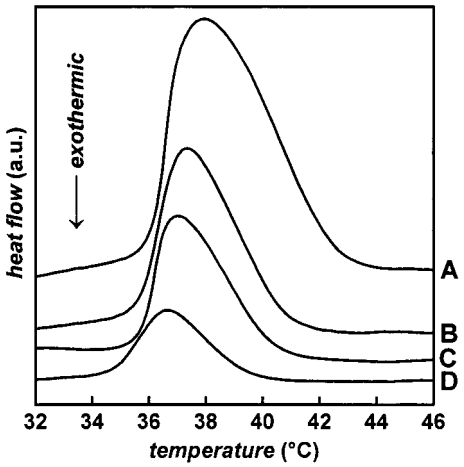

Figure 10. Differential scanning calorimetry (DSC) diagrams of the transition of the hexagonal phase to the lamellar phase in the samples A−D (see Figure 5). The analytical data are given in Table 1.

to the overall sample weight also systematically depends on the relative amount of the hexagonal phase in the respective sample. Figure 10 shows the DSC diagrams of the four samples A−D. The plots are normalized with respect to the overall sample weights. It is noticeable that for higher relative amounts of the hexagonal phase the temperature interval in which the phase transition occurs is wider and slightly shifted toward higher temperatures. The calorimetric data are given in Table 1.

Conclusions

In addition to the formerly reported synthesis in aqueous systems, mesostructured aluminophosphate/dodecyl phosphate composite materials are also successfully prepared in alcoholic media. This synthesis has a highly cooperative mechanism, since any mesostructures in the reaction mixtures are formed only after the addition of the inorganic reactant to the surfactant/alcohol solution; the pure surfactant/alcohol systems are not lyotropic. As long as the reaction temperature is kept low, the products consist of two phases, one of which is lamellar. The other phase has an inverted hexagonal structure, which is thermally unstable; at ∼35−43 °C it transforms into the lamellar structure. The lamellar structure is formed exclusively if the synthesis is carried out at higher temperatures, although it has a less well-ordered structure than a lamellar phase prepared under aqueous conditions. In-situ SAXS investigations demonstrate that the reaction proceeds slower in alcoholic media than in water and that the product composition systematically changes in dependence of both the synthesis temperature and the reaction time.

Acknowledgment. We thank Deutsche Forschungsgemeinschaft (Fr1372/1-1) and Fonds der Chemischen Industrie for financial support. M.T. thanks the Freie und Hansestadt Hamburg for a Ph.D. scholarship.

CM991165D